molecule, the σ charge donated from the carbon atom was found to be larger than the π charge accepted,[31] thus affirming the importance of the σ electron charge.

The nature of the bonding of atoms together into a molecular unit is examined in this paper from the viewpoint of the final electronic structure. While interesting and important from other views, changes in charges and bonding as bonds are formed are not relevant to the viewpoint here and so are not considered. The question considered here is, What are the energy contributions (σ and π) to the total electronic energy of the molecule in its stable molecular state?

The main point of this paper is to point out the importance of the σ electrons to the stability of the metal-carbon bond of transition metal carbonyls, including chemisorbed CO. In the consideration of the relative roles of σ and π electrons, the π electrons have received the most attention. This occurs because the π electrons generally have the highest energies and therefore are the most readily shifted. The π electron shifts produced by changing the surface site of chemisorbed CO (on-top vs bridge bonding) and the effect of other adsorbents on CO are reflected in large shifts in the C-O infrared stretching frequency and adsorption binding energies. There is a large amount of literature in this area. The importance of the CSOV approach is that it shows that charge reorganization is necessary to form a stable bond between CO and a metal and that, of the various types of reorganization, the shifting of the π electrons makes the largest contribution to stability. The importance of the separation of the total calculated energy into monatomic and diatomic energy terms presented here is that it shows that after the charge reorganization has occurred, the largest contribution to the stability of the metal-carbon bond is provided by the σ electrons. It is the attraction of the σ electrons to the metal and carbon atoms that provides the largest share of the glue (cohesive energy) that constitutes the metal-carbon bond. This is shown using, for the first time, an energy criterion rather than the more qualitative bond order criterion.

Acknowledgment is made to the donors of the Petroleum Research Fund, administered by the American Chemical Society, for partial support of this research and to the University of Arkansas for a computing time grant.

Registry No. CO, 630-08-0; Fe, 7439-89-6.

(32) Barnes, L. A.; Bauschlicher, C. W., Jr. *J. Chem. Phys.* **1989**, *91*, 314.
(33) Barnes, L. A.; Rosi, M.; Bauschlicher, C. W., Jr. *J. Chem. Phys.* **1991**, *94*, 2031.

Ziegler-Natta Catalysis. A Theoretical Study of the Isotactic Polymerization of Propylene

L. A. Castonguay and A. K. Rappé*

Contribution from the Department of Chemistry, Colorado State University, Fort Collins, Colorado 80523. *Received December 16, 1991*

Abstract: The stereotacticity of *ansa*-zirconium metallocene Ziegler-Natta propylene polymerization catalysts is studied using a combination of ab initio electronic structure techniques and empirical force field molecular mechanics techniques. The experimental observation of isotacticity for the *rac*-(1,2-ethylenebis(η^5-indenyl)zirconium and *rac*-(1,2-ethylenebis(η^5-tetrahydroindenyl)zirconium based catalysts is computationally reproduced, and an explanation for the reduced rate of reaction and the atacticity for the *meso*-(1,2-ethylenebis(η^5-indenyl))zirconium catalysts is provided. In addition, modified *rac*-(1,2-ethylenebis(η^5-tetrahydroindenyl))zirconium catalysts with predicted increased isotacticity and decreased isotacticity (despite the presence of a chiral metal center), respectively, are proposed. Further, a new catalyst is proposed which should yield syndiotactic polypropylene.

I. Introduction

Homogeneous catalysts are actively being studied as useful reagents for the stereospecific Ziegler-Natta polymerization of propylene. Isotactic polypropylene has been produced using active catalysts derived from chiral, *ansa*-metallocene compounds of group 4 transition metal elements and methylaluminoxane ($[Al(CH_3)-O]_n$) (MAO) cocatalysts.[1] The discovery of a highly isotactic (ethylenebis(tetrahydroindenyl))$ZrCl_2$/MAO, catalytic system (Figure 1, A) by Kaminsky, Brintzinger, and co-workers[2] and a highly syndiotactic isopropyl(cyclopentadienyl-1-fluorenyl)$ZrCl_2$/MAO catalytic system (Figure 1, B) by Ewen and co-workers[3] has prompted further research into the effects of ligand on stereoregulation.[4]

In general, Ziegler-Natta catalysts produce syndiotactic, isotactic, or atactic polypropylenes. These three types of polymer have differing relative orientations of the chiral centers which occur at alternate positions along the polymer chain (Figure 2). Isotactic polypropylene has the same relative configuration at all of the chiral centers (the methine carbons) and is commercially important owing to its greater tensile strength.[6] Syndiotactic polypropylene has a regular alternation of configuration at adjacent chiral centers along the polymer chain, and atactic polypropylene has a ster-

(1) (a) Kaminsky, W., Sinn, H., Eds. *Transition Metals and Organometallics as Catalysts for Olefin Polymerization*; Springer-Verlag: Berlin, 1980. (b) Quirk, R. P., Ed. *Transition Metal Catalyzed Polymerizations; Ziegler-Natta and Metathesis Polymerizations*; Cambridge University Press: Cambridge, 1988.
(2) Kaminsky, W.; Kulper, K.; Brintzinger, H. H.; Wild, F. R. W. P. *Angew. Chem., Int. Ed. Engl.* **1985**, *24*, 507.
(3) Ewen, J. A.; Jones, R. L.; Razavi, A. *J. Am. Chem. Soc.* **1988**, *110*, 6255.
(4) (a) Corradini, P.; Geurra, G.; Vacatello, M.; Villani, V. *Gazz. Chim. Ital.* **1988**, *118*, 173. (b) Roll, W.; Brintzinger, H. H.; Rieger, B.; Zolk, R. *Angew. Chem., Int. Ed. Engl.* **1990**, *29*, 279. (c) Collins, S.; Gauthier, W. J.; Holden, D. A.; Kuntz, B. A.; Taylor, N. J.; Ward, D. G. *Organometallics* **1991**, *10*, 2061. (d) Cavallo, L.; Guerra, G.; Vacatello, M.; Corradini, P. *Macromolecules* **1991**, *24*, 1784. (e) Longo, P.; Proto, A.; Grassi, A.; Ammendola, P. *Macromolecules* **1991**, *24*, 4624.
(5) Pino, P.; Cioni, P.; Wei, J.; Rotzinger, B.; Arizzi, S. In *Transition Metal Catalyzed Polymerizations; Ziegler-Natta and Methasis Polymerizations*; Quirk, R. P., Ed.; Cambridge University Press: Cambridge, 1988; p 1 and references therein.
(6) Collman, J. P.; Hegedus, L. S.; Norton, J. R.; Finke, R. G. *Principles and Applications of Organotransition Metal Chemistry*; University Science Books: Mill Valley, CA, 1987.

0002-7863/92/1514-5832$03.00/0

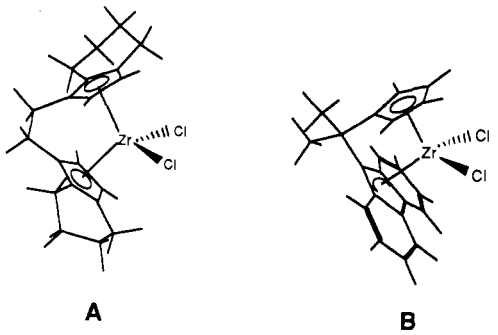

Figure 1. (*S,S*)-C_2H_4(4,5,6,7-tetrahydro-1-indenyl)$_2ZrCl_2$ (A) and (*i*-PrCp-1-Flu)$ZrCl_2$ (B).

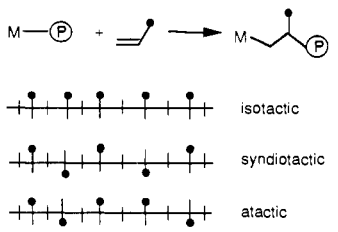

Figure 2. Types of vinyl olefin polymer tacticity.

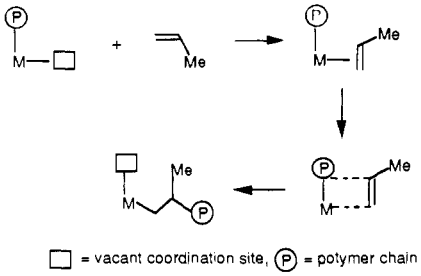

Figure 3. Cossee mechanism for Ziegler–Natta olefin polymerization.

eorandom distribution of the chiral centers.

The most widely accepted mechanism for Ziegler–Natta olefin polymerization is the Cossee mechanism[7] (Figure 3), though modifications invoking effects such as α-agostic hydrogen interactions have been proposed.[8] In the Cossee mechanism, a vacant coordination site is generated initially, followed by olefin complexation. Formal migration of the polymer chain, P, and formation of the metal–carbon bond occur concertedly through a four-center transition state. This recreates a vacant coordination site at the site originally occupied by the polymer chain and the process continues; the growing polymer chain terminus flips from side to side.

There are two proposed types of stereocontrol: stereochemical control by the chirality of the catalyst (enantiomorphic site control)[9] and stereochemical control by the configuration (chirality) of the last inserted monomer unit (chain end control).[10] Stereochemical control in syndiotactic polymerization of propylene by soluble vanadium catalysts obeys the chain end control model.[11] Group 4B *ansa*-metallocene compounds (with MAO) produce

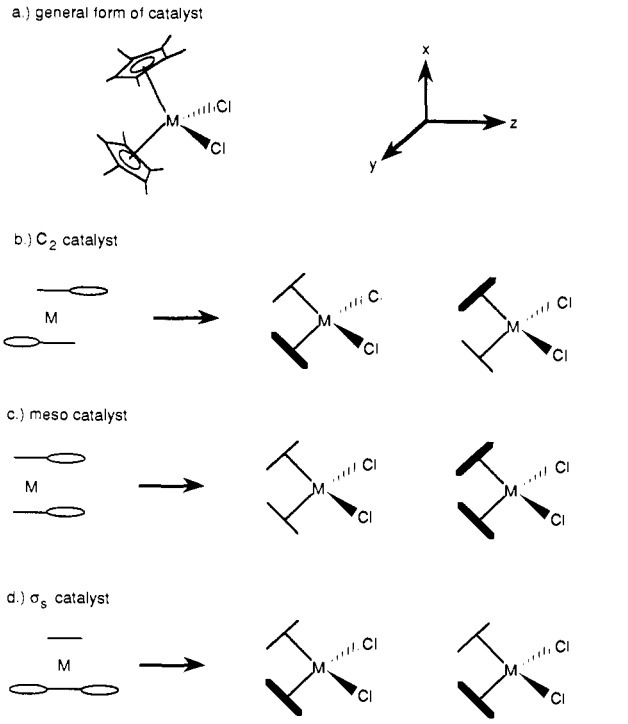

Figure 4. General symmetric forms for *ansa*-metallocene catalysts and definition of notation.

isotactic polypropylene dominantly by an enantiomorphic site control mechanism.[12]

Before the 1980's, propylene polymerizations with group 4B bis(cyclopentadienyl)M^{IV} derivatives, where M is Ti or Zr, and MAO cocatalysts yielded only atactic polymer.[13] In 1984, Ewen reported the first example of a bis-Cp catalyst that yielded isotactic polymer.[12a] The catalyst, $Cp_2Ti(Ph)_2$, and MAO cocatalyst produces isotactic polypropylene by a chain end control mechanism. Enantiomeric racemic forms of ethylene bridged indenyl titanocene derivatives yield isotactic polypropylene by the enantiomorphic site control model. Atactic polypropylene is produced by the ethylene bridged titanium indenyl meso diastereomer and achiral Cp_2ZrCl_2 zirconocene derivatives. Recently Erker reported chiral, nonbridged bis-Cp Zr catalysts which produce isotactic polypropylene through a mixture of chain end control and enantiomorphic site control.[12c]

The current catalysts used in the homogeneous isotactic polymerization of propylene are of the general form Cp_2ML_2 in which the Cp ligands are stereoselectively substituted. It is generally acknowledged that the steric environment around the metal contributes to the orientation of the insertion of the monomer into the M–C bond and ultimately the tacticity (enantiomorphic site control).[1,4,12] The parent (unsubstituted) catalyst has C_{2v} symmetry, and one can classify the symmetric catalysts with substitution of the Cp ligands such that the C_{2v} symmetry is disrupted as containing either the C_2 axis of symmetry or one of the two mirror planes (meso or σ_s) found in the C_{2v} point group. This symmetry notation will be shown below to be useful in differentiating the morphology of the "active site" of the possible catalysts and the tacticity that the catalysts are likely to yield.

The notation of Figure 4 for the stereochemistry at the metal center will be used in the following analysis. The general (unsubstituted) catalyst along with the conventional C_{2v} coordinate system is shown in Figure 4a. Symmetric catalysts with substitution of the Cp ligands such that the C_{2v} symmetry is disrupted contain either a C_2 axis of symmetry or one of the two mirror

(7) (a) Cossee, P. *J. Catal.* **1964**, *3*, 80. (b) Arlman, E. J.; Cossee, P. *J. Catal.* **1964**, *3*, 99.

(8) Brookhardt, M.; Green, M. L. H. *J. Organomet. Chem.* **1983**, *250*, 395. Clawson, L.; Soto, J.; Buchwald, S. L.; Steigerwald, M. L. *J. Am. Chem. Soc.* **1985**, *107*, 3377. Burger, B. J.; Thompson, M. E.; Cotter, W. D.; Bercaw, J. E. *J. Am. Chem. Soc.* **1990**, *112*, 1566. Piers, W. E.; Bercaw, J. E. *J. Am. Chem. Soc.* **1990**, *112*, 9406. Roll, W.; Brintzinger, H.-H.; Rieger, B.; Zolk, R. *Angew. Chem., Int. Ed. Engl.* **1990**, *29*, 279. Krauledat, H.; Brintzinger, H.-H. *Angew. Chem., Int. Ed. Engl.* **1990**, *29*, 1412.

(9) (a) Sheldon, R. A.; Fueno, T.; Tsunstsugu, T.; Kurukawa, J. *J. Polym. Sci., Part B* **1965**, *3*, 23. (b) Doi, Y.; Asakuru, T. *Makromol. Chem.* **1975**, *176*, 507.

(10) Bovey, F. A.; Tiers, G. V. D. *J. Polym. Sci.* **1960**, *44*, 173.

(11) (a) Zambelli, A.; Locatelli, P.; Zannoni, G.; Bovey, F. A. *Macromolecules* **1978**, *11*, 923. (b) Zambelli, A.; Locatelli, P.; Provasoli, A.; Ferro, D. R. *Macromolecules* **1980**, *13*, 267.

(12) (a) Ewen, J. A. *J. Am. Chem. Soc.* **1984**, *106*, 6355. (b) Pino, P.; Cioni, P.; Wei, J. *J. Am. Chem. Soc.* **1987**, *109*, 6189. (c) Erker, G.; Nolte, R.; Aul, R.; Wilker, S.; Kruger, C.; Noe, R. *J. Am. Chem. Soc.* **1991**, *113*, 7594.

(13) (a) Pino, P.; Mulhaupt, R. *Angew. Chem., Int. Engl.* **1980**, *19*, 857. (b) Sinn, H.; Kaminsky, W. *Adv. Organomet. Chem.* **1980**, *18*, 99.

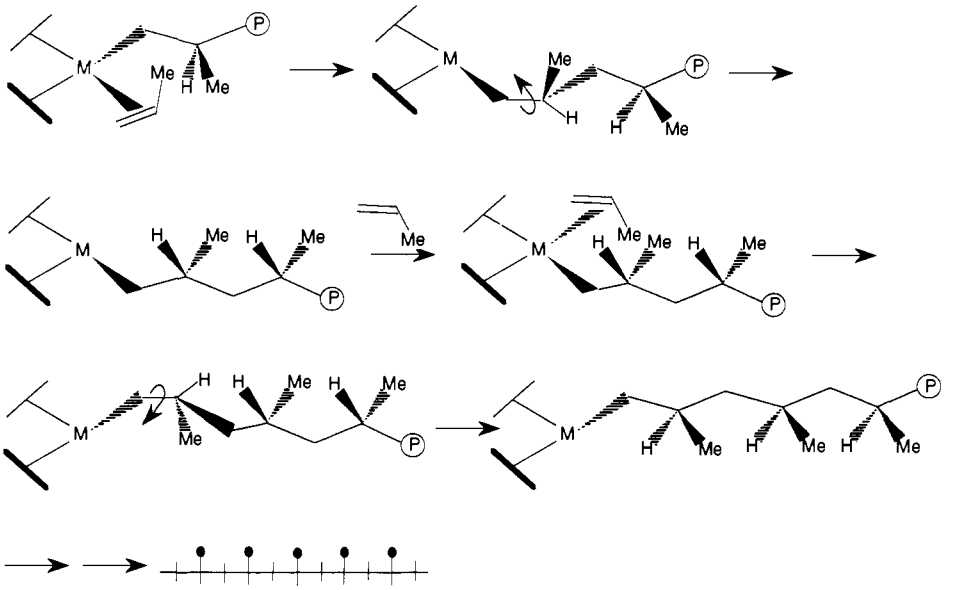

Figure 5. Reaction sequence for isotactic propylene polymerization.

planes (meso or σ_s). Schematic representations are shown in Figure 4, b, c, and d, respectively. Views looking down the z-axis and also looking down and up the y-axis, respectively, are shown. An example of a C_2 catalyst is the (*S*,*S*)-(ethylenebis(tetrahydroindenyl))$ZrCl_2$ (Figure 1, A), and an example of a meso catalyst is the meso form of this catalyst, *meso*-(ethylenebis(tetrahydroindenyl))$ZrCl_2$. The isopropyl(cyclopentadienyl-1-fluorenyl)$ZrCl_2$ catalyst shown in Figure 1, B, is an example of a σ_s catalyst.

The isotactic polymerization of propylene (Cossee mechanism) as suggested by Pino and co-workers[5] is shown in detail in Figure 5. The initial olefin complexation occurs with the methyl group being placed in the least sterically congested quadrant. Olefin insertion occurs and the C_α–C_β bond is formally rotated to standard form. The second olefin complexation occurs, again placing the methyl group in the least sterically congested quadrant. Olefin insertion and formal rotation occurs leaving the polymer in standard form. As mentioned above, the terminus of the growing polymer chain flips from side to side.

Analysis of defects in the isotactic polymer chain can provide useful information regarding the mechanism of stereocontrol. Isotactic polypropylene and two types of defects are shown in Figure 6. The isotactic polymerization of propylene proceeds by primary insertion of propylene into the metal–polymer bond.[12] Subsequent reactions of propylene occur from the same prochiral face (Figure 5). A syndiotactic defect occurs when propylene reacts from the opposite prochiral face. A secondary defect, which produces a polymer with two adjacent methine units, occurs by secondary insertion of propylene.

Computational models for site control of stereoregularity in Ziegler–Natta catalysis have been limited to rigid model calculations in which only a limited number of torsional angles are varied.[4a] As a first step in the theoretical characterization of stereospecific Ziegler–Natta polymerization catalysts, we report an ab initio study for a zirconium catalyst model system and a molecular mechanics study of the well-known isotactic catalyst, (*S*,*S*)-C_2H_4(4,5,6,7-tetrahydro-1-indenyl)$_2ZrCl_2$, the corresponding slower atactic meso catalyst, another known isotactic catalyst, (*S*,*S*)-C_2H_4-bis(indenyl)$ZrCl_2$, and two modified (*S*,*S*)-C_2H_4-(4,5,6,7-tetrahydro-1-indenyl)$_2ZrCl_2$ catalysts, one of which should yield increased isotacticity and one which should yield atactic polymer. Further, a new catalyst is proposed which should yield syndiotactic polypropylene.[14]

The theoretical methodology utilized is discussed in the Theoretical Details section below. The computational results are presented in the Results and Discussion section, and the overall conclusions are presented in the Summary and Conclusions section.

II. Theoretical Details

A. Ab Initio Calculations. All calculations were carried out using Cartesian–Gaussian basis sets. For Cl[15] an effective core potential was used to replace the core electrons, and for Zr[16] an effective potential was used to replace the 1s, 2s, 2p, 3s, 3p, and 3d orbitals. A Dunning–Huzinaga[17] (9s5p/3s2p) basis set was used for carbon. A (4s/2s) basis set, scaled, was used for hydrogen.[17] For chlorine, a valence double basis (3s, 3p/2s, 2p)[15] was used for all calculations. For Zr[16] a Hay–Wadt valence double-ζ (5s5p4d/3s3p2d) basis set was used. The geometries of the stationary points were generated with analytic gradient techniques using Hartree–Fock wave functions.

Following the geometry optimizations, the basis was augmented by the addition of a set of d functions to each carbon center, $\zeta = 0.75$. GVB pairs were formed for the active bond pairs (Zr–C and C–C σ and π) leading to a GVB(3/6) wave function, and a full CI was carried out within this six orbital space (GVB–CI).

B. Molecular Mechanics and Dynamics Calculations. Force Field. Recent reports on the application of molecular mechanics to organometallic chemistry include a number of studies of cyclopentadienyl complexes.[18-20] For this class of compounds, recent studies[19,20] have included a pseudoatom at the centroid of the Cp ring with the metal attached to this pseudo atom. The steric effect of a *tert*-butyl group attached to a cyclopentadienyl ligand on the conformational preference of the cyclopentadienyl ring for [(η^5-$C_5H_4Bu^t$)Fe(CO)(L)I] complexes has been studied.[19] The steric contribution to the olefin hydrogenation at an organoactinide site was studied[20] using an augmented Dreiding force field.[21] From the papers it appears that the metal–Cp unit was forced to be rigid in each case.

The Dreiding force field[21] was extended in this work to include an atom type for tetrahedral zirconium and pseudoatoms for a cyclopentadienyl centroid (Cp), an η^3-π-allyl centroid (Pi), and an olefin centroid (Ci) (Figure 7). The parameters for the remaining atoms were taken directly from the published Dreiding force field. For zirconium, a covalent radius of 1.54 Å was used. For the Cp, Pi, and Ci pseudoatoms, covalent radii of 0.74 Å each were used, and these radii are used to determine the natural bond lengths for all bonds to zirconium.

(14) For additional details, see: L. A. Castonguay, Ph.D. Thesis, Colorado State University, Nov 1991.

(15) Rappé, A. K.; Smedley, T. A.; Goddard, W. A. *J. Phys. Chem.* **1981**, *85*, 1662.
(16) Hay, P. J.; Wadt, W. R. *J. Chem. Phys.* **1985**, *82*, 270.
(17) Dunning, T. H.; Hay, P. J. *Modern Theoretical Chemistry: Methods of Electronic Structure Theory*; Schaefer, H. F., III Ed.; Plenum Press: New York, 1977; Vol. 3, p 1. Huzinaga, S. *J. Chem. Phys.* **1965**, *42*, 1293.
(18) (a) Menger, F. M.; Sherrod, M. J. *J. Am. Chem. Soc.* **1988**, *110*, 8606. (b) Thiem, H.-J.; Brandl, M.; Breslow, R. *Ibid.* **1988**, *110*, 8612.
(19) du Plooy, K. E.; Marais, C. F.; Carlton, L.; Hunter, R.; Boeyens, J. C. A.; Coville, N. J. *Inorg. Chem.* **1989**, *28*, 3855.
(20) Lin, Z.; Marks, T. J. *J. Am. Chem. Soc.* **1990**, *112*, 5515.
(21) Mayo, S. L.; Olafson, B. D.; Goddard, W. A. *J. Phys. Chem.* **1990**, *94*, 8897.

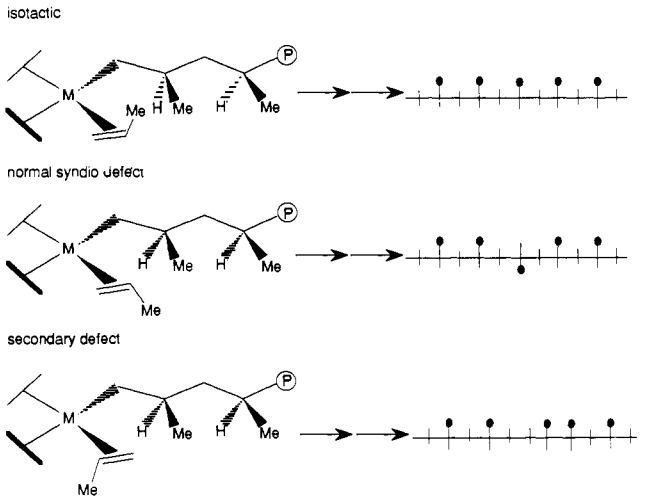

Figure 6. Stereodefects in an isotactic polymer chain.

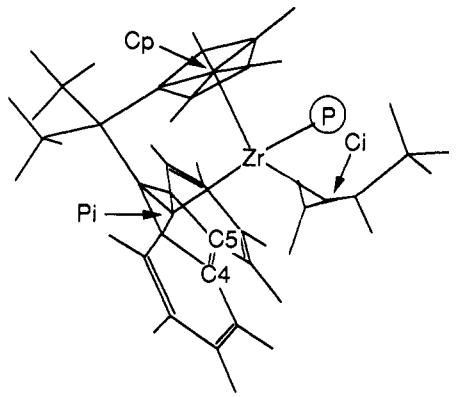

Figure 7. Geometric definitions of the Cp, Pi, and Ci pseudoatom types.

Table I. Angle Parameters

angle[a]	force constant, (kcal/mol)/rd^2	equilibrium angle, (deg)
Ci–C_2–C_2	0	
C_2–Ci–C_x	100	90
C_2–Ci–C_2	0	
Cp–C_R–X	100	180
Pi–C_R–X	100	180
C_R–Cp–X	100	90
C_R–Pi–X	100	90
Cp–C_R–C_R	0	
Pi–C_R–C_R	0	
C_R–C–C_R	0	
C_R–Pi–C_R	0	
X–Zr–X	100	109.4710

[a] C_2 = olefinic carbon, C_R = aromatic carbon, X = all other nondefined atoms, Zr = zirconium.

Pseudoatoms to cyclopentadienyl and olefinic cabons were set so that reasonable cyclopentadienyl ring and olefin carbon distances were produced. The bond length between Ci and an olefinic carbon was set to 0.667 Å, so that the natural carbon–carbon double bond length of 1.324 Å was retained. The bond lengths between a cyclopentadienyl carbon and Cp or Ci are set to 1.1824 and 0.9951, respectively. For zirconium a natural tetrahedral angle of 109.471° was used with a force constant of 100 (kcal/mol)/rd^2. The angle parameters used are listed in Table I.

The torsional terms for two bonds IJ and KL connected via a common bond JK was chosen to be of the form:

$$E_\phi = \tfrac{1}{2}V_\phi[1 + d\cos(n\phi)] \quad (1)$$

where V_ϕ is one-half the rotational barrier in kcal/mol, n is the periodicity of the potential, and d (+1 or −1) is the phase factor. The rule-based scheme as outlined in the Dreiding force field paper[18] was used for the new pseudoatom types and zirconium. The torsional parameters used are listed in Table II.

Table II. Torsional Parameters

torsion[a]	V_j	n	d
Ci–C_2–C_2–X	0		
X–Zr–C_3–X	2	3	−1
X–Ci–C_2–X	1	4	−1
X–C_i–C_2–C_2	0		
C_2–C_i–C_2–X	0		

[a] C_3 = alkyl carbon, C_2 = olefinic carbon, C_R = aromatic carbon, X = all other nondefined atoms, Zr = zirconium.

Table III. Ab Initio Structural Results

distance (Å) or angle (deg)	ground state	act. complex	transition state	product
Zr–C_1	2.90	2.55	2.18	2.14
Zr–C_2	2.40	2.54	2.66	2.97
Zr–C_3	2.14	2.28	2.42	2.95
C_1–C_2	1.36	1.36	1.46	1.57
C_2–C_3	3.52	2.91	2.02	1.57
Zr–C_1–C_2	55.0	74.0	91.9	105.5
C_1–C_2–C_3	133.8	124.0	115.1	117.6
Zr–C_3–C_2	42.0	57.0	73.0	75.5

Table IV. Ab Initio Energies: Total Energy for Reactants (hartrees) and Relative Energy for Complexes (kcal/mol)

wave function	reactants	gs complex	transition state	product
HF, no pol.	−1082.4378	−37	−15	−26
HF, pol.	−1082.4774	−37	−15	−28
GVB(3/6), pol.	−1082.5388	−33	−10	−24
GVB-CI, pol.	−1082.526	−33	−9	−20

The partial charges were determined using the recently developed *QEq* charge equilibration scheme.[22] Nonbonded interactions (van der Waals forces) are included in the Dreiding force field, using a Lennard-Jones type expression:

$$E_{vdw} = D_{ij}\{-2[x_{ij}/x]^6 + [x_{ij}/x]^{12}\} \quad (2)$$

where D_{ij} is the well depth in kcal/mol and x_{ij} is the van der Waals bond length in Å. For zirconium, a bond length of 4.60 Å and a well depth of 0.555 were used. van der Waals interactions at pseudoatoms Cp, Ci, and Pi were ignored.

For calculations involving a fluorenyl ligand, the following changes in the force field were made. The Zr–Cp distance was set to 2.1 Å and the Zr–Pi distance was set to 2.25 Å. The Cp–C_R–C_3 and Pi–C_R–C_3 angles were set to 180° with force constants of 10 (kcal/mol)/rd^2; C_3 denotes an alkyl carbon. The Zr–C_R nonbond off-diagonal distance was set to 2.25 Å with a well depth of 2.0 kcal/mol.

For pentane, octane, and toluene, the solid state molecular mechanics minimization used the crystal coordinates and cell parameters obtained from the Cambridge Data Bank as the trial guess. Electrostatic interactions were summed over a 5 × 5 × 5 grid in real space and then continued periodically with Ewald sums. During minimization, the coordinates of the molecules in the unit cell, as well as the unit cell, were optimized.

Procedure. All of the reported molecular mechanics calculations were carried out using the Biograf and Polygraf molecular simulation programs,[23] Version 2.2. In order to address the large number of conformational degrees of freedom available in the complexes studied, the minimized charge equilibrated trial structure for each complex discussed in the Results and Discussion section below was subjected to 10–20 cycles of annealed dynamics from 0 to 600 K with a symmetric temperature ramp of 1° per 1 fs. Each structure from the resulting collection of structures was minimized using a Fletcher–Powell minimization procedure, and the charges were reequilibrated. The lowest energy structure from each set was then subjected to the same process until no new lower energy structures were found.

During all mechanics and dynamics calculations, all atomic and pseudoatomic positions were varied and the olefin was constrained to be parallel to the Zr–polymer bond using a torsional constraint of 1000 kcal/mol. For calculations involving the fluorenyl ligand, two additional

(22) Rappé, A. K.; Goddard, W. A. *J. Phys. Chem.* **1991**, *95*, 3358.
(23) Biograf and Polygraf obtained from the BioDesign subsidiary of Molecular Simulations Inc., 199 S. Los Robles Ave., Suite 540, Pasadena, CA 91101.

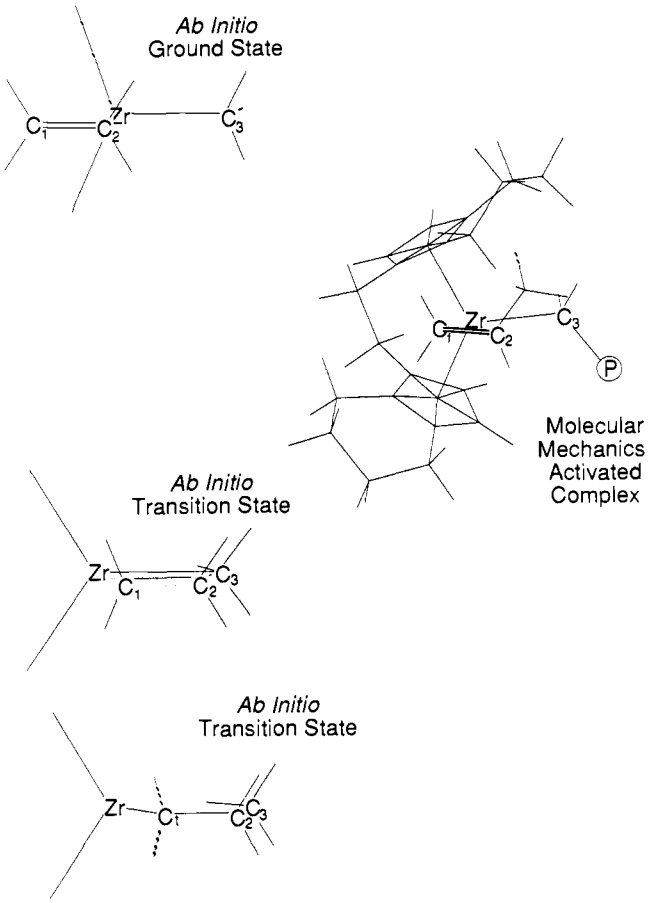

Figure 8. Ab initio geometric structures and molecular mechanics activated complex.

distance constraints were used: Zr–C(4) and Zr–C(5) distances were constrained to 2.584 Å with distance constraints of 1000 (kcal/mol)/Å^2.

III. Results and Discussion

A. Ab Initio Calculations. In order to probe the electronic rearrangements which occur along the reaction coordinate for zirconium-catalyzed olefin polymerization and establish an activated complex (AC) structure to be used in the molecular mechanics calculations, the ground, transition, and product states of the model system, $Cl_2ZrCH_3^+ + C_2H_4 \rightarrow Cl_2ZrC_3H_7^+$ were determined by ab initio electronic structure techniques (Figures 8–10 and Tables III and IV).

The orbital reorganization common to the theoretical studies of metal-containing four-center 2 + 2 reactions published to date[24,25] is as follows:

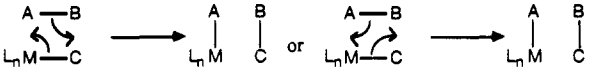

The bond between centers A and B in the reactant is converted into a bond between centers B and C in the product. In response to this, the bond between M and C in the reactant is transformed into a bond between centers M and A in the product. Independent of the direction of electron flow there are always two centers (M and B or A and C) whose one-electron orbitals remain on their original centers and two centers whose one-electron orbitals move during the course of reaction. If "symmetry" (e.g., ethylene plus ethylene or ethylene plus formaldehyde) precludes this localization, the reactions have a high activation energy.[24e,f]

It is generally accepted[26,27] that the insertion of metal–ligand σ bonds into C–C π bonds occurs through a prior coordination of the π bond onto the metal center followed by a $2\pi + 2\sigma$ reaction involving the C–C π bond and the metal ligand σ bond. The general analysis given above and by Thorn and Hoffmann[26] is found to be operative here.

For $Cl_2ZrCH_3^+ + C_2H_4$, we find the saddlepoint for ethylene insertion to be rather late; the Zr–C_1 bond distance of 2.18 Å is only 0.04 Å longer than in the final product. The lateness of the transition state is due to the large binding energy of ethylene to the cationic Zr complex (33 kcal/mol; see Table IV) which makes the reaction from π complex to propyl product endothermic by 13 kcal/mol (with respect to the π complex). This excessive binding energy is due to a combination of several effects including (1) a lack of the counterion which would dissipate the polarization of ethylene by the charged complex (the calculations are carried out effectively in the gas phase), (2) a lack of solvent which would again dissipate the polarization of ethylene by the charged complex and would undoubtedly be bound to the complex in the absence of olefin, and (3) the presence of the sterically smaller Cl's rather than the observed Cp's. The calculated energetics, as given in Table IV, are rather insensitive to addition of polarization functions and inclusion of electron correlation.

The valence orbitals for the reactant ethylene complex (Figure 9a–d, column 1) are as would be expected for a weak Lewis acid–base complex since the metal center lacks an appropriate pair of electrons for Dewar–Chatt–Duncanson backbonding.[27] The π bond pair between C_1 and C_2 involved in the Lewis acid–base interaction is plotted in Figure 9, a and b, column 1; the delocalization onto the metal center is small. The Zr–C σ bond pair is plotted in Figure 9, c and d, column 1. The carbon one-electron orbital is in Figure 9c and the Zr d_σ orbital is plotted in Figure 9d. As the ethylene moves toward (Figure 9a–d, column 2) and then to the transition state (Figure 9a–d, column 3), the p orbital on C_2 moves to Zr to form the Zr–C_1 σ bond (see Figure 9b, columns 2 and 3). The p orbital on C_1 remains on C_1 and rehybridizes to form the sp^x orbital involved in the Zr–C_1 σ bond (see Figure 9a, columns 2 and 3). The Zr d_σ orbital originally involved in the σ bond between Zr and C_3 moves to C_2 to form the C_2–C_3 σ bond in the product. The one-electron orbital on C_3 remains on C_3 and merely rotates in going from being bound to Zr to being bound to C_2. The remaining electronic distortion in going from the transition state to the product is rather small, again being indicative of a late transition state.

As discussed above, two of the four orbitals do remain on their initial atomic centers (C_1 and C_3) during the reaction and two do flow across (from C_2 to Zr and from Zr to C_2) in response to bonding changes that occur during the reaction.

Similar calculations on the analogous titanium system have been reported in the literature.[28] The transition states for both the titanium and zirconium systems have the metal–C1 distance substantially shortened and the metal–C3 distance lengthened as the olefin inserts into the metal–methyl bond. These calculations lend further support to the Cossee mechanism in which the polymer flips from side to side.

As is apparent from the structures in Figure 8, the Zr center is significantly pyramidal in the reactant as well as in the propyl product. The barrier for inversion at Zr (analogous to the inversion at nitrogen form ammonia) for $Cl_2ZrCH_3^+$ is calculated (with

(24) (a) Steigerwald, M. L.; Goddard, W. A. *J. Am. Chem. Soc.* **1984**, *106*, 308–311. (b) Upton, T. H. *J. Am. Chem. Soc.* **1984**, *106*, 1561–1571. (c) Fujimoto, H.; Yamasaki, T.; Mizutani, H.; Koga, N. *J. Am. Chem. Soc.* **1984**, *106*, 6157–6161. (d) Koga, N.; Obara, S.; Kitaura, K.; Morokuma, K. *J. Am. Chem. Soc.* **1984**, *106*, 7109–7116. (e) Rappé, A. K.; Upton, T. H. *Organometallics* **1984**, *3*, 1440–1442. (f) Upton, T. H.; Rappé, A. K. *J. Am. Chem. Soc.* **1985**, *107*, 1206–1218. (g) Koga, N.; Obara, S.; Kitaura, K.; Morokuma, K. *J. Am. Chem. Soc.* **1985**, *107*, 7109–7116. (h) Rabaâ, H.; Sailard, J.-Y.; Hoffmann, R. *J. Am. Chem. Soc.* **1986**, *108*, 4327–4333. (i) Rappé, A. K. *Organometallics* **1987**, *6*, 354–357. (j) Williamson, R. L.; Hall, M. B. *J. Am. Chem. Soc.* **1988**, *110*, 4428–4429.

(25) Rappé, A. K. *Organometallics* **1990**, *9*, 466.

(26) Thorn, D. L.; Hoffmann, R. *J. Am. Chem. Soc.* **1978**, *100*, 2079–2090.

(27) Albright, T. A.; Burdett, J. K.; Whangbo, M.-H. *Orbital Interactions in Chemistry*; Wiley: New York, 1985. Collman, J. P.; Hegedus, L. S.; Norton, J. R.; Finke, R. G. *Principles and Applications of Organotransition Metal Chemistry*; University Science Books: Mill Valley CA, 1987.

(28) (a) Novaro, O.; Blaisten-Barojas, E.; Clementi, E.; Giunchi, G.; Ruiz-Vizcaya, M. E. *J. Chem. Phys.* **1978**, *68*, 2337. (b) Fujimoto, H.; Yamasaki, T.; Mitzutani, H.; Koga, N. *J. Am. Chem. Soc.* **1985**, *107*, 6157. (c) Jolly, C. A.; Marynick, D. S. *J. Am. Chem. Soc.* **1989**, *111*, 7968.

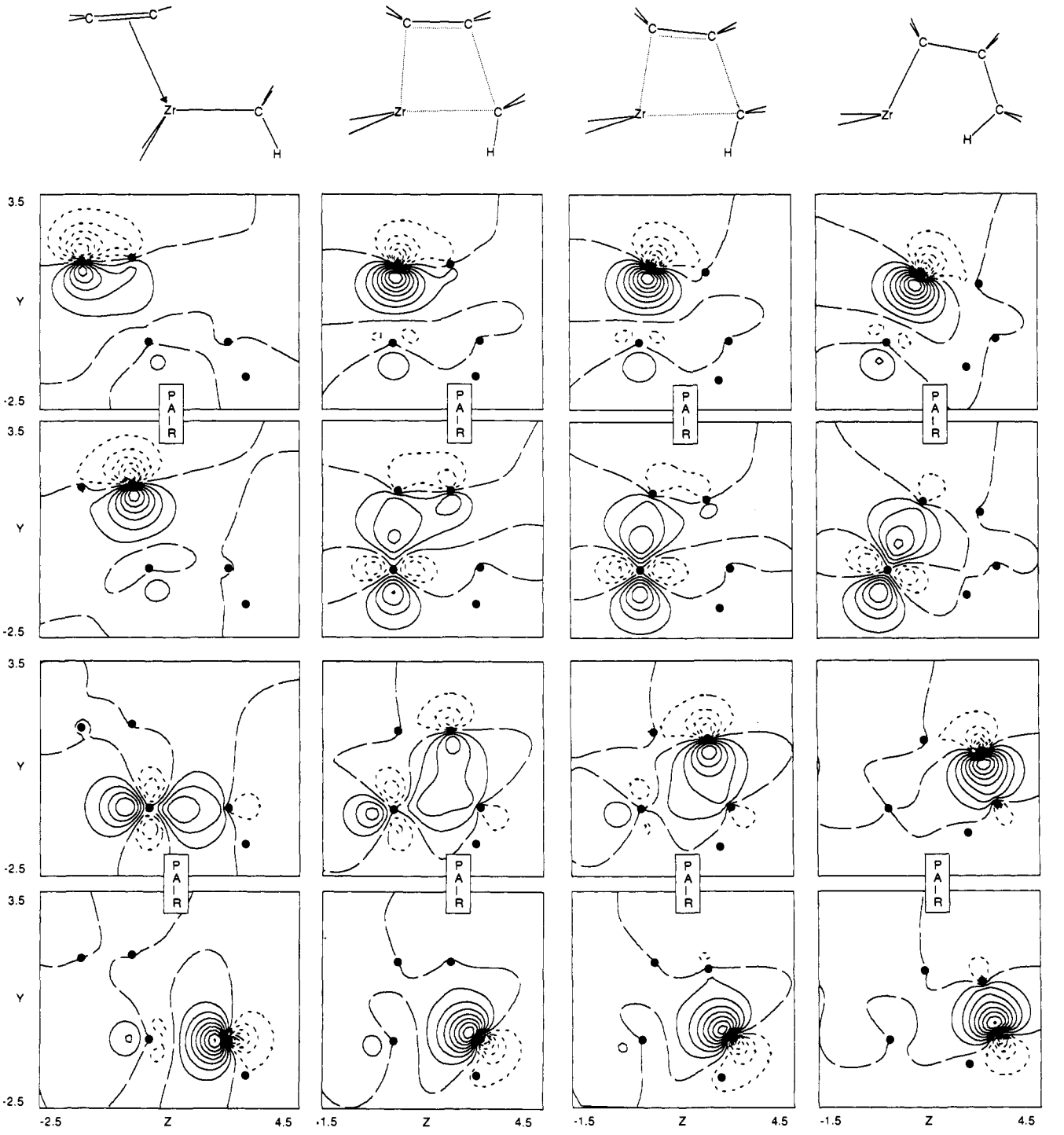

Figure 9. Contour plots of the GVB orbitals defining the one-electron orbitals of the two active pairs as a function of position along the reaction coordinate. The plotting plane for each orbital contains all of the active centers (Zr, the three carbons, and one hydrogen). The solid contours define positive orbital amplitude (spaced 0.0625 a.u.), the dashed contours define negative orbital amplitude, and the long dashed lines define nodal lines. The first column contains the C_1–C_2 π bond and the Zr–C_3 σ bond of the reactant. The second column displays the corresponding orbitals for a complex ~0.4 Å prior to the transition state. The rearranged Zr–C_1 σ bond and C_2—C_3 σ bond orbitals of the transition state are plotted in the third column. The corresponding product orbitals are shown in the fourth column.

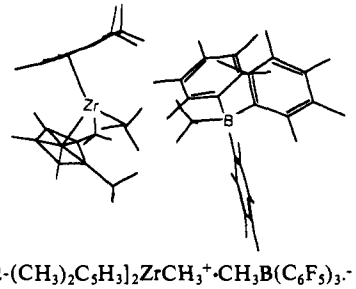

Figure 10. $[1,2\text{-}(CH_3)_2C_5H_3]_2ZrCH_3^+ \cdot CH_3B(C_6F_5)_3^-$

a Hartree–Fock wave function) to be 3.5 kcal/mol. Previous ab initio calculations[28b,c,29] have also shown the ground state geometries for Ziegler–Natta model systems, $Cl_2TiCH_3^+$, $Cl_2TiCH_3^+$, and $Cl_2ZrCH_3^+$, to be nonplanar but that the barriers to inversion are small. A 3-kcal/mol inversion barrier for $Cl_2TiCH_3^+$ was reported by Marynick.[29]

(29) Jolly, C. A.; Marynick, D. S. *Inorg. Chem.* **1989**, *28*, 2893.
(30) (a) Grassi, A.; Zambelli, A.; Resconi, L.; Albizzati, E.; Mazzocchi, R. *Macromolecules* **1988**, *21*, 617. (b) Grassi, A.; Ammendola, P.; Longo, P.; Albizzati, E.; Resconi, L.; Mazzocchi, R. *Gazz. Chim. Ital.* **1988**, *118*, 539.

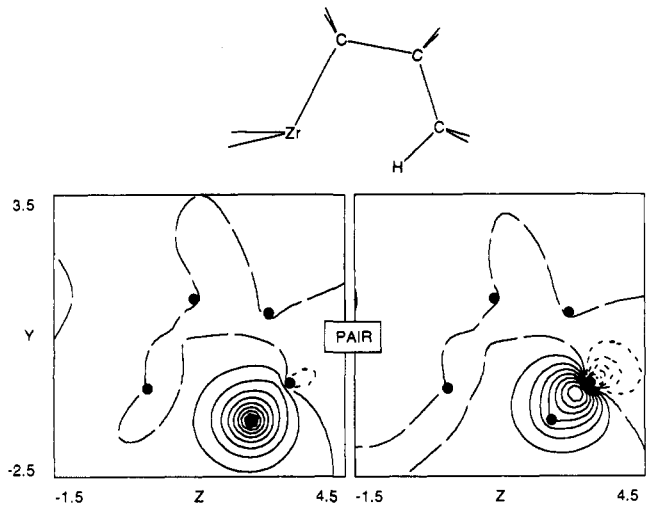

Figure 11. Contour plots of the GVB orbitals defining the one-electron orbitals of the C–H bond "complexed" to Zr. The plotting plane for each orbital contains all of the active centers (Zr, the three carbons, and one hydrogen). The solid contours define positive orbital amplitude (spaced 0.0625 a.u.), the dashed contours define negative orbital amplitude, and the long dashed lines define nodal lines.

Because of the size of the tetrahydroindenyl catalyst of interest, molecular mechanics calculations were used to estimate the inversion barrier for the tetrahydroindenyl catalyst. The calculated inversion barrier for the second insertion THI complex is 5 kcal/mol, and hence the metal center is not likely to be the source of a significant inversion barrier.

Recently, Marks reported the synthesis and the X-ray crystal structure of a "cation-like" zirconocene polymerization catalyst, $[1,2\text{-}(CH_3)_2C_5H_3]_2ZrCH_3^+ \cdot CH_3B(C_6F_5)_3^-$ (Figure 10) with an observed inversion barrier of 18.3 kcal/mol.[31] To probe the effect of counterion and indirectly the effect of solvation on the inversion barrier, the barrier to inversion for the Marks' "cation-like" catalyst was determined. The calculated inversion barrier is 10–11 kcal/mol (two pathways for inversion were considered). This method underestimates the inversion barrier, but can certainly be used for a rough estimate. To probe the effect of counterion, the inversion barrier was calculated without the presence of counterion and was found to be 4 kcal/mol. These results suggest that the inversion barrier is increased when counterion is present and that differential (due to differing dipole and higher moments) solvation is also important.

Additionally, for the propyl product there is a significant interaction between the Zr center and one of the hydrogens bound to C_3. The Zr–H distance is 2.25 Å and the C–H distance has increased 0.05 Å from 1.08 Å to 1.13 Å. Further, the initially formed fully eclipsed conformation is isoenergetic with a fully staggered conformation (the HF without d polarization functions, but geometrically optimized total energies are within 1 kcal/mol). This is suggestive of an agostic interaction; however, the one-electron orbitals for the C–H bond pair plotted in Figure 11 suggest otherwise. There is not a significant delocalization of the C–H orbitals onto the Zr center; the interaction is electrostatic in nature.

B. Molecular Mechanics Calculations. To test the utility of empirical force field molecular mechanics techniques in the "design" of new catalysts for stereocontrolled propylene polymerization, calculations were carried out on three known *ansa*-metallocene catalysts as well as three proposed catalysts. The results on the three known systems are presented first followed by the results on three predicted systems.

1. (*S*,*S*)-C_2H_4(4,5,6,7-tetrahydro-1-indenyl)$_2ZrCl_2$. To test the utility of the augmented force field for the prediction of tacticity, calculations were carried out on the reported[2] highly isotactic catalyst, (*S*,*S*)-C_2H_4(4,5,6,7-tetrahydro-1-indenyl)$_2ZrCl_2$ (Figure 1). The literature experimental results are for the racemic form of the catalyst.

(31) Yang, X.; Stern, C. L.; Marks, T. J. *J. Am. Chem. Soc.* **1991**, *113*, 3623.

Table V. Geometric Results for THI Propylene Complex

geometric parameter	distance (Å) or angle (deg)
Zr–Cp centroid	2.32
Zr–Cp carbons (average)	2.71
Zr–polymer carbon	2.31
Zr–olefin centroid	2.33
Zr–olefin carbons	2.51
Cp–Zr–Cp	114.8
polymer–Zr–olefin centroid	106.6

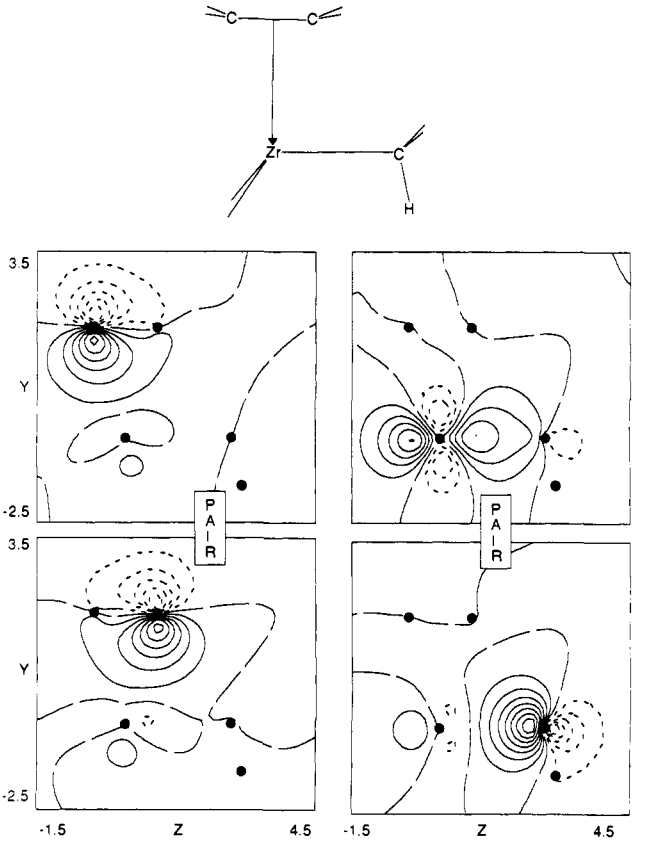

Figure 12. Contour plots of the GVB orbitals defining the one-electron orbitals of the two active pairs for the "activated complex" used in the molecular mechanics calculations. The plotting plane for each orbital contains all of the active centers (Zr, the three carbons, and one hydrogen). The solid contours define positive orbital amplitude (spaced 0.0625 a.u.), the dashed contours define negative orbital amplitude, and the long dashed lines define nodal lines.

Molecular mechanics calculations were performed on an AC of the (*S*,*S*)-tetrahydroindenyl (THI) catalyst system approximately halfway along the reaction pathway between ground state and transition state (Figure 8). In the AC, the Zr–C_1 distance was chosen to be 2.5 Å and the Zr–C_2 distance was chosen to be 2.5 Å. Geometric parameters for the first coordination sphere of zirconium are collected in Table V. From a comparison of the orbital plots in Figure 9, column 1, with the orbital plots in Figure 12, this activated complex is electronically only slightly perturbed from the reactant π complex. Molecular mechanics and annealed dynamics calculations were run in order to find the lowest energy conformations of the proposed activated complexes (see Procedure section above).

For the first insertion, where P = Me, the difference in energy (ΔE) between the AC leading to a syndiotactic defect and one leading to an isotactic chain extension is calculated to be a little less than 3 kcal/mol; the complex leading to isotactic polymer is favored. The polymer chain length dependence on the energy differential was studied by determining the energetics of the

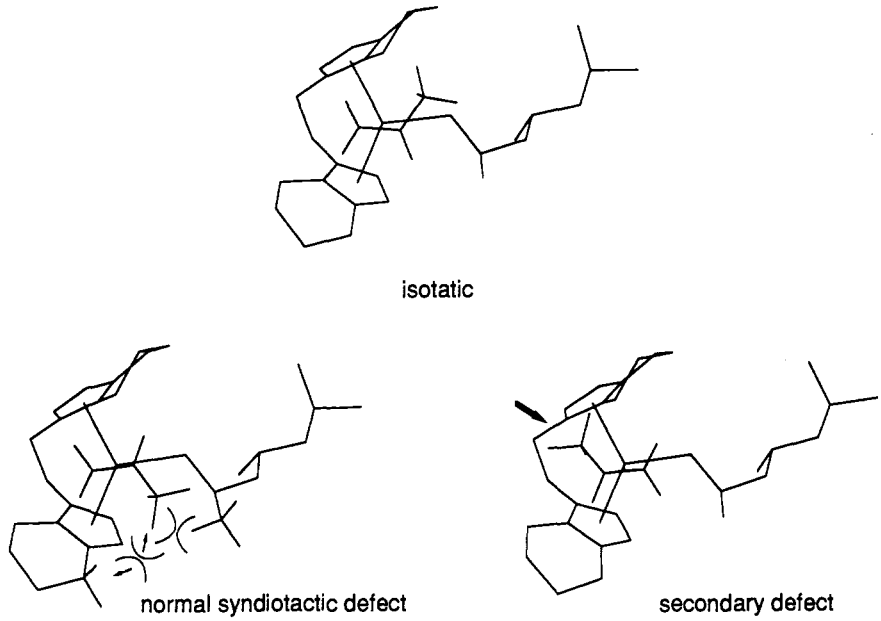

Figure 13. Calculated structures for the third insertion for the THI activated complexes. Hydrogens not involved in differential steric interactions have been removed for clarity.

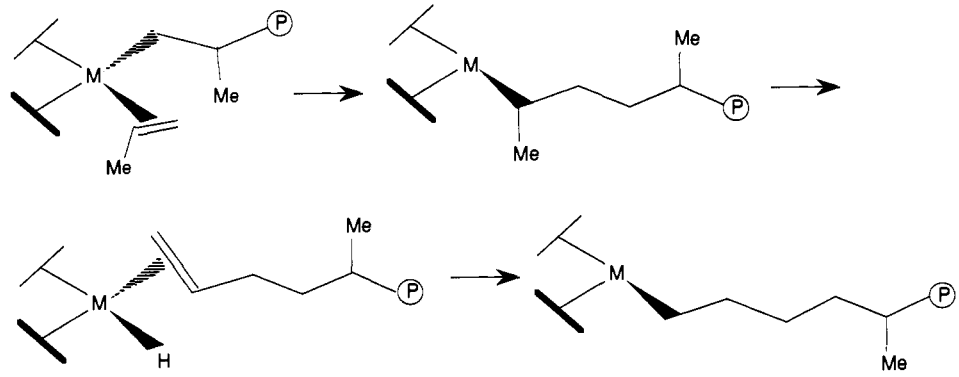

Figure 14. Reaction sequence leading to a 1–3 insertion defect.

activated complexes for the second and third insertions as well. For the second insertion, the AC leading to isotactic polymer is favored by 6 kcal/mol over the AC leading to a syndiotactic defect, and by a little less than 6 kcal/mol over the AC leading to a secondary defect. For the third insertion, the AC leading to isotactic polymer is favored by 5 kcal/mol over both the AC's leading to a syndiotactic defect and to a secondary defect. The AC's are shown in Figure 13 with the unfavorable steric interactions marked with arrows. The AC leading to isotactic polypropylene is favored for one, two, and three insertions, and therefore we conclude that the calculated tacticity does not significantly depend on polymer length after the initial insertion step. Further, we conclude that, since there is an energetic differential between the first insertion (3 kcal/mol) and subsequent insertions (5 to a little over 6 kcal/mol), the isotacticity is at least partially due to a double stereodifferentiation.[12c]

Experimentally, the defects that are observed are syndiotactic defects and, to a lesser extent, secondary defects and a defect that results in a four methylene sequence. This four methylene sequence has been attributed to 1,3-propylene insertion, resulting from secondary insertion, followed by β-hydride elimination and subsequent primary insertion of the polymer vinyl end group into the M–H bond (Figure 14).[30]

2. (*S*,*S*)-C_2H_4-bis(indenyl)$ZrCl_2$. The racemic bis(indenyl) catalyst yields isotactic polypropylene experimentally.[4c] For the first insertion the AC leading to isotactic polypropylene is favored by 1 kcal/mol over the AC leading to a syndiotactic defect (Figure 15). This result agrees with the known experimental tacticity. This differential is smaller than that observed for the *rac*-THI system discussed above (3 kcal/mol) but is still significant.

3. *meso*-C_2H_4(4,5,6,7-tetrahydro-1-indenyl)$_2ZrCl_2$. Experimentally, the meso catalyst yields atactic polymer, but at a much slower rate than the *rac*-THI catalyst.[4c] Because of the puckering of the cyclohexyl rings, no symmetry exists in this catalyst, and therefore calculations have been carried out with the olefin complexed to each of the two enantiotopic faces and in both possible primary insertion geometries (methyl up versus methyl down). These four AC's for the first insertion are shown in Figure 16. The two conformations in which the olefin is complexed on the face opposite the cyclohexyl groups, Figure 16, c and d, are favored and are nearly the same energy. The other two conformations in which propylene is on the same side as the cyclohexyl groups are approximately 5–6 kcal/mol higher in energy. These results suggest that there is no preference for whether the methyl is up or down in the propylene leading to atactic polymer, but that there is substantial preference for olefin complexation to the side without cyclohexyl groups. Since the polymer flips from side to side during polymerization (and the barrier to inversion is larger; vide supra) and, therefore, the olefin complexes at alternating sides, the rate for this catalyst should be much slower than for *rac*-THI.

4. Proposed Modifications of (*S*,*S*)-C_2H_4(4,5,6,7-tetrahydro-1-indenyl)$_2ZrCl_2$. To test the usefulness of the present force field methodology in the design of new catalysts and to provide straightforward experimental tests of the molecular mechanics results, the AC's in Figure 13 were examied at a graphics screen, and two sites for methyl substitution were chosen: one which would increase te stereoselectivity and one which would decrease the stereoselectivity. The first substitution placed a methyl group in the 4-position of the cyclohexyl group (Figure 17). Putting a methyl substitution there raises the AC (third insertion case)

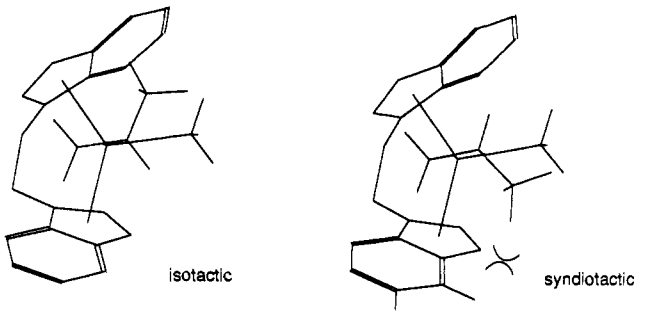

Figure 15. Calculated structures for the first insertion for the C_2H_4-bis(indenyl)$ZrCl_2$ activated complexes. Hydrogens not involved in differential steric interactions have been removed for clarity.

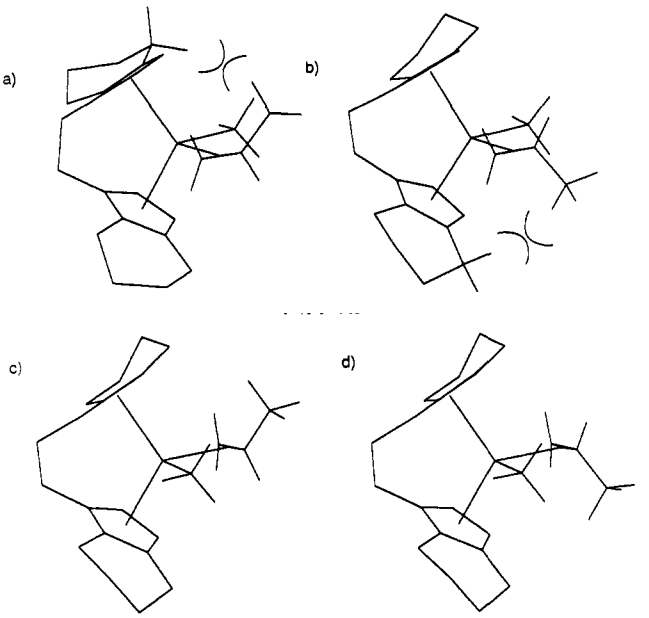

Figure 16. Calculated structures for the first insertion for the *meso*-C_2H_4(4,5,6,7-tetrahydro-1-indenyl)$_2ZrCl_2$ activated complexes. Hydrogens not involved in differential steric interactions have been removed for clarity.

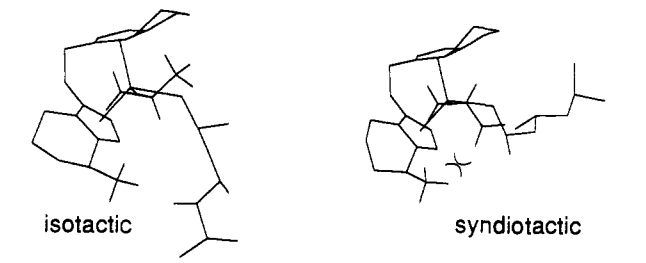

Figure 17. Calculated structures for the first insertion for the proposed modification of THI catalyst for increased isotacticity. Hydrogens not involved in differential steric interactions have been removed for clarity.

energy differential by an additional kilocalorie/mole, making the ΔE between the syndiotactic defect AC and the isotactic AC 6 kcal/mol (compared to 5 kcal/mol for *rac*-THI). Placing the methyl group in this position sterically congests the space where the propylene methyl group sits for the AC leading to a syndiotactic defect. We predict that this substitution should lessen the number of syndiotactic defects, which are the major defect type for this catalyst.

The second substitution placed a methyl group in the 3-position of the Cp ligand (Figue 18). This substitution should lead to atactic polymer. The AC's leading to isotactic polymer and a syndiotactic defect for the third insertion case are almost of equal energy. Putting the methyl group in this position sterically congests the space where the propylene methyl group sits for the AC leading

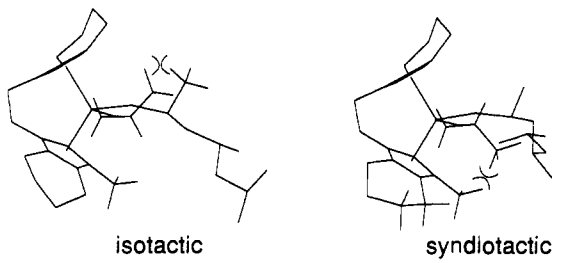

Figure 18. Calculated structures for the first insertion for the proposed modification of THI catalyst leading to atactic polymer. Hydrogens not involved in differential steric interactions have been removed for clarity.

to a syndiotactic defect. For the isotactic AC, the methyl substitution causes steric congestion between the propylene methyl and the polymer chain. The polymer chain moves away from the substituted methyl to minimize the unfavorable methyl–methyl interaction, but doing so places it near the propylene methyl. The syndiotactic AC is only 1 kcal/mol higher than the isotactic AC. For the parent (*S*,*S*) THI case, the difference is 5 kcal/mol.

5. Proposed Syndiotactic σ_s Catalyst. Syndiotactic polypropylene has a regular alternation of configuration at adjacent chiral centers along the polymer chain (Figure 2). A reaction sequence which is consistent with syndiotactic polymerization of propylene (Cossee mechanism) is shown in detail in Figure 19. The initial olefin complexation occurs with the methyl group being placed in the least sterically congested quadrant. Olefin insertion occurs and the C_α–C_β bond is rotated to standard form. The second olefin complexation occurs again, placing the methyl group in the least sterically congested quadrant. Olefin insertion and formal rotation occur, leaving the polymer in standard form. As mentioned previously, the terminus of the growing polymer chain flips from side to side. The syndiotactic polymerization of propylene in this mechanism proceeds by primary insertion of propylene into the metal–polymer bond. Subsequent reactions of propylene occur at alternating opposite prochiral faces.

If polymerization takes place by the Cossee mechanism, then a correlation exists between the idealized symmetry (Figure 4) of the catalyst and the tacticity of the polymer produced. Propylene complexation occurs with the methyl group being placed in the least sterically congested quadrant. This process determines the stereochemistry (tacticity) of the growing polymer chain. *rac*-THI and C_2H_4-bis(indenyl)$ZrCl_2$, C_2 catalysts, yield isotactic polymer due to the steric interactions of propylene with the indenyl ligands. These interactions cause the conformation in which the propylene methyl group is on the same face as the indenyl ligand to be unfavorable. A C_2 catalyst should produce isotactic polymer (Figure 5). A meso catalyst should produce atactic polymer and *meso*-THI does. The two conformations in which propylene is complexed on the face opposite the indenyl cyclohexyl groups with either methyl up or down are favored. Since there is no preference for whether the methyl is up or down, atactic polymer is produced. If the olefin complexation occurs at alternating sides as polymerization proceeds, a σ_s catalyst should yield syndiotactic polymer since the same propylene conformations (i.e., Me up or Me down) would be favored as the polymer chain grows and the polymer terminus flips from side to side. Reaction would occur with alternant prochiral faces. This demands the barrier to inversion to be high compared to the barrier to propagation.

We propose, and Marks finds,[31] the barrier to inversion to be large for *ansa* metallocene complexes, and, thus, we propose tht C_2H_4[cyclopentadienyl-1-6,7,8,9,10,11,12,13-octahydrofluorenyl]$ZrCl_2$, a σ_s catalyst, would yield syndiotactic polypropylene. As in the *meso*-THI case, no symmetry exists due to the puckering of the cyclohexyl rings, and therefore all four combinations for the first insertion were calculated (Figure 20). The two conformations in which the propylene methyl is up but bound on opposite prochiral faces are favored. This would correspond to the formation of syndiotactic polypropylene.

6. Isopropyl(cyclopentadienyl-1-fluorenyl)$ZrCl_2$. Ewen reported the syndiotactic polymerization of propylene with isopropyl(cy-

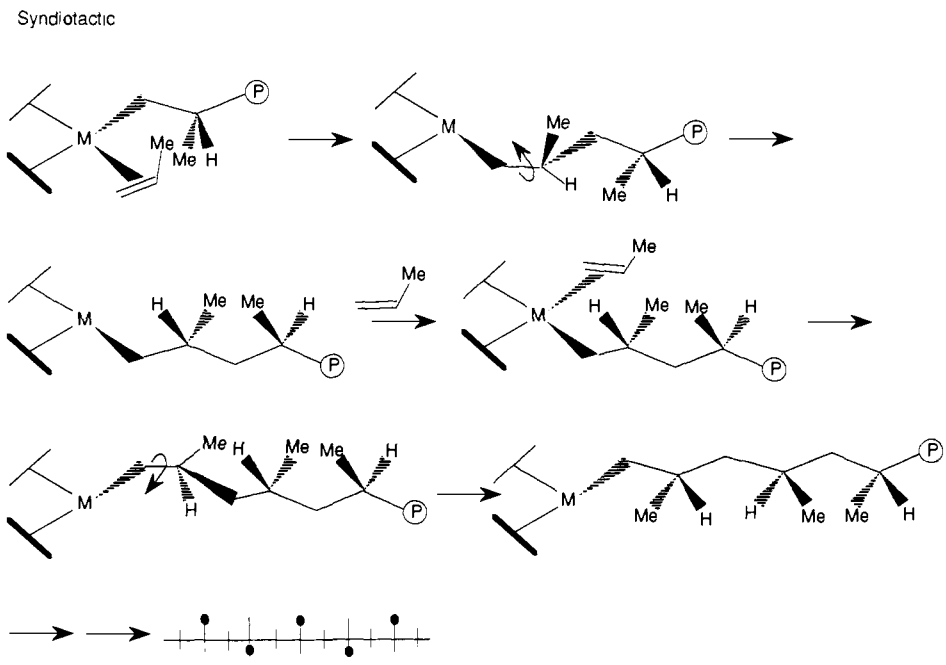

Figure 19. Reaction sequence for a proposed syndiotactic catalytic cycle.

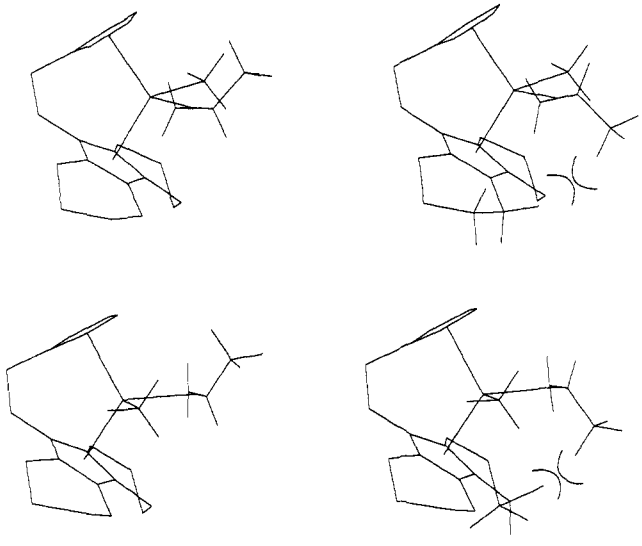

Figure 20. Calculated structures for the first insertion for a proposed syndiotactic σ_s catalyst. Hydrogens not involved in differential steric interactions have been removed for clarity.

clopentadienyl-1-fluorenyl)$ZrCl_2$/MAO (Figure 1).[3] Having correctly predicted isotacticity for the THI catalyst among other indenyl isotactic and atactic catalysts, the same methodology was applied to a known syndiotactic σ_s catalyst, *i*-PrCp-1-Flu$ZrCl_2$. For the first insertion AC, both conformations (propylene methyl up and down) are calculated to have the same energy. For the third insertion, the AC leading to an isotactic defect is favored over the AC leading to syndiotactic polypropylene by a little less than 2 kcal/mol. These results contradict experiment. The steric interaction which should differentiate between the conformations is between the methyl group of propylene and the aryl group of the fluorenyl ligand. To test the adequacy of the *present* force field for alkyl–alkyl and alkyl–aryl interactions, calculations were carried out on a crystals of pentane, octane, and toluene.[32] With the Dreiding force field the energies of sublimations for pentane and octane are in error by 0.1 kcal/mol and −0.4 kcal/mol, respectively. For toluene the energy of sublimation is in error by −1.65 kcal/mol. For pentane the lattice constants (Å) are (experimental values in parentheses): a = 4.31 (4.10), b = 9.05 (9.04), and c = 15.07 (14.70). For octane the lattice constants (Å) are (experimental values in parentheses): a = 4.36 (4.16), b = 4.71 (4.75), and c = 11.06 (11.00). For toluene the lattice constants (Å) are (experimental values in parentheses): a = 7.814 (7.666), b = 5.845 (5.832), and c = 26.858 (26.980). The energies of sublimation and lattice constants for pentane and octane are in good agreement with experiment. For toluene, though the agreement with experimental lattice constants is good, the magnitude of the error in the heat of sublimation is of the same magnitude as the ΔE of interest, and, therefore, further improvement in the force field is needed in order to investigate this fluorenyl system. It should be noted that the proposed σ_s syndiotactic catalyst, C_2H_4[cyclopentadienyl-1-6,7,8,9,10,11,12,13-octahydrofluorenyl]$ZrCl_2$, does not contain aryl–alkyl interactions and therefore the calculations are valid.

(32) Anderson, M.; Bosio, L.; Bruneaux-Poulle, J.; Fourme, R. *J. Chim. Phys.* **1977**, *74*, 68.

Summary and Conclusions

The electronic reorganization reported previously for other organometallic reactions was found for olefin insertion into a Zr–methyl σ bond. An augmentation of the Dreiding force field to include zirconium and centroids for olefins, η^3-π-allyls, and cyclopentadienyl rings was presented. This force field was applied to an investigation of the origin of tacticity in the Ziegler–Natta polymerization of propylene. The ground and transition states of the model system, $Cl_2ZrCH_3^+ + C_2H_4 \rightarrow Cl_2ZrC_3H_7^+$, were determined by ab initio techniques. In the transition state for the zirconium system, the metal–C1 distance shortens and the metal–C3 distance lengthens as the olefin inserts into the metal–methyl bond. These calculations lend further support to the Cossee mechanism in which the polymer flips from side to side. Molecular mechanics calculations were carried out on activated complexes of Ziegler–Natta indenyl catalysts approximately halfway along the reaction pathway between ground state and transition state. The effect of polymer chain length was studied for the isotactic catalyst, (*S*,*S*)-C_2H_4(4,5,6,7-tetrahydro-1-indenyl)$_2ZrCl_2$. The correct tacticity is found computationally, and no dependence of tacticity on polymer length is found beyond the first insertion. Catalyst modifications to improve isotacticity are proposed. Other catalysts that were studied were the corresponding meso catalyst and C_2H_4-bis(indenyl)$ZrCl_2$. The correct tacticities are calculated for both, atactic and isotactic, respectively. A new syndiotactic catalyst is proposed, C_2H_4[cyclopentadienyl-1-(6,7,8,9,10,11,12,13-octahydrofluorenyl)]$ZrCl_2$.

The major factors affecting the tacticity include the symmetry of the catalyst dictated by the steric environment of the ancillary ligands. Olefin complexation occurs with the methyl group being placed in the least sterically congested quadrant, and this process continues, ultimately determining the stereochemistry of the growing polymer chain. This lends further support to enantiomorphic site control of chirality. Since there is an energetic differential between the first insertion (3 kcal/mol) and subsequent insertions (5 to 6 kcal/mol), the isotacticity is at least partially due to a double stereodifferentiation.[12c]

Acknowledgment. We thank Molecular Simulations Inc., for the use of the Biograf and Polygraf molecular simulation programs. Parital support of this research by Shell Development is gratefully acknowledged. This research was partially supported by a grant (GM39038) from the National Institutes of Health. A.K.R. gratefully acknowledges helpful discussions with Drs. W. M. Skiff, S. E. Wilson, and P. N. Haxin of Shell Development.

Design of Chromophoric Molecular Assemblies with Large Second-Order Optical Nonlinearities. A Theoretical Analysis of the Role of Intermolecular Interactions

Santo Di Bella,† Mark A. Ratner,* and Tobin J. Marks*

Contribution from the Department of Chemistry and the Materials Research Center, Northwestern University, Evanston, Illinois 60208-3113. *Received December 30, 1991*

Abstract: The role and nature of intermolecular interactions in determining quadratic nonlinear optical macroscopic hyperpolarizabilities are investigated using the INDO/S (ZINDO) sum-over excited particle-hole-states formalism on clusters (dimers and trimers) of archetypical donor/acceptor organic π-electron chromophore molecules. It is found that the calculated aggregate hyperpolarizability depends strongly on relative molecular orientations, exhibiting the largest values in slipped cofacial arrangements, where the donor substituent of one molecular unit is in close spatial proximity to the acceptor substituent of the nearest neighbor. These results convey important suggestions for the design of multichromophore assemblies having optimum $\chi^{(2)}$ values. For example, cofacial assembly of chromophores having low ground-state dipole moments should maximize molecular contributions to the macroscopic susceptibility. The classical "two-level" model is a good approximation for estimating the hyperpolarizability in such cluster systems, although at larger distances it yields overestimated β_{ijk} values. Other cases where the two-level model breaks down more significantly are also identified.

Introduction

Materials exhibiting large nonlinear optical (NLO) responses, in particular those composed of conjugated organic chromophore molecules, have attracted much recent scientific interest.[1-3] The attraction of incorporating them into devices for technological applications has stimulated efforts in the design and synthesis of new chromophoric building blocks and multimolecular assemblies.[2,3] The concurrent desirability of having a proper, chemically-oriented, physical description of molecular NLO phenomena has led to the parallel development of quantum chemical approaches for calculating optical nonlinearities.[4-7] To date these approaches have, however, been largely limited to the calculation of the *molecular* nonlinear response in order to rationalize and optimize single chromophore quadratic hyperpolarizabilities.[4-7] The important relationship between microscopic and macroscopic second-order NLO properties has only been addressed for macroscopic systems (e.g., crystals,[8] poled polymers,[9] assembled layer thin films[10]) using local field factor corrections that phenomenologically approximate, via empirical polarizabilities, molecule–molecule interactions and the effects of molecular packing on the molecular hyperpolarizability.[11-14]

An alternative computational approach for estimation of nonadditive interchromophore effects would be to consider a molecular cluster representative of the crystal environment to calculate the effective hyperpolarizability. In this case, in place of electrostatic corrections, it should be possible to define, via reliable electronic structure formalism, the role and nature of intermolecular interactions that determine the bulk hyperpolarizability and ultimately to use this information for the design of new materials. The aims of the present work are to explore systematically, for the first time in any detail,[15] the second-order nonlinear response of simple clusters (dimers and trimers) of

† Permanent address: Dipartimento di Scienze Chimiche, Universitá di Catania, 95125 Catania, Italy.

(1) (a) Boyd, R. W. *Nonlinear Optics*; Academic Press: New York, 1992. (b) Prasad, N. P.; Williams, D. J. *Introduction to Nonlinear Optical Effects In Molecules and Polymers*; Wiley: New York, 1991. (c) Shen, Y. R. *The Principles of Nonlinear Optics*; Wiley: New York, 1984.

(2) (a) *Materials for Nonlinear Optics: Chemical Perspectives*; Marder, S. R., Sohn, J. E., Stucky, G. D., Eds.; ACS Symposium Series 455; American Chemical Society: Washington, DC, 1991. (b) *Nonlinear Optical Properties of Organic Materials III*; Khanarian, G., Ed. *SPIE Proc.* **1990**, *1337*. (c) *Nonlinear Optical Properties of Organic Materials II*; Khanarian, G., Ed. *SPIE Proc.* **1990**, *1147*. (d) *Nonlinear Optical Effects in Organic Polymers*; Messier, J., Kajar, F., Prasad, P., Ulrich, D., Eds.; Kluwer Academic Publishers: Dordrecht, 1989. (e) *Organic Materials for Nonlinear Optics*; Hann, R. A., Bloor, D., Eds.; Royal Society of Chemistry: London, 1988. (f) *Nonlinear Optical Properties of Organic Molecules and Crystals*; Chemla, D. S., Zyss, J., Eds.; Academic Press: New York, 1987; Vols. 1 and 2. (g) *Nonlinear Optical Properties of Organic and Polymeric Materials*; Williams, D. J., Ed.; ACS Symposium Series 233; American Chemical Society: Washington, DC, 1984.

(3) (a) Eaton, D. F. *Science* **1991**, *253*, 281. (b) Marder, S. R.; Beratan, D. N.; Cheng, L.-T. *Science* **1991**, *252*, 103. (c) Zyss, J. *J. Mol. Electron.* **1985**, *1*, 25. (d) Williams, D. J. *Angew. Chem., Intl. Ed. Engl.* **1984**, *23*, 690.

(4) Ab initio: (a) Karna, S. P.; Prasad, P. N.; Dupuis, M. *J. Chem. Phys.* **1991**, *94*, 1171. (b) Meyers, F.; Adant, C.; Bredas, J. L. *J. Am. Chem. Soc.* **1991**, *113*, 3715. (c) Rice, J. E.; Amos, R. D.; Colwell, S. M.; Handy, N. C.; Sanz, J. *J. Chem. Phys.* **1990**, *93*, 8828. (d) Dykstra, C. E.; Jasien, P. G. *Chem. Phys. Lett.* **1984**, *109*, 388. (e) Sekino, H.; Bartlett, R. J. *J. Chem. Phys.* **1986**, *85*, 976; *Int. J. Quantum Chem.*, in press.

(5) CNDO/S: (a) Morley, J. O. *J. Chem. Soc., Faraday Trans.* **1991**, *87*, 3009, 3015. (b) Morley, J. O. *J. Am. Chem. Soc.* **1988**, *110*, 7660. (c) Docherty, V. J.; Pugh, D.; Morley, J. O. *J. Chem. Soc., Faraday Trans. 2* **1985**, *81*, 1179. (d) Lalama, S. J.; Garito, A. F. *Phys. Rev.* **1979**, *20*, 1179. (e) Morrell, J. A.; Albrecht, A. C. *Chem. Phys. Lett.* **1979**, *64*, 46.

(6) PPP: (a) Li, D.; Ratner, M. A.; Marks, T. J. *J. Phys. Chem.*, in press. (b) Li, D.; Ratner, M. A.; Marks, T. J. *J. Am. Chem. Soc.* **1988**, *110*, 1707. (c) Li, D.; Marks, T. J.; Ratner, M. A. *Chem. Phys. Lett.* **1986**, *131*, 370. (d) Dirk, C. W.; Twieg, R. J.; Wagniere, G. *J. Am. Chem. Soc.* **1986**, *108*, 5387. (e) Soos, Z.; Ramasesha, S. *J. Chem. Phys.* **1989**, *90*, 1067.

0002-7863/92/1514-5842$03.00/0